A COUPLED HYDRAULIC AND ELECTRICAL STRESS DETERMINATION TECHNIQUE

Mai Linh DOAN
Département de Sismologie, Institut de Physique du Globe de Paris, France

François H. CORNET
Département de Sismologie, Institut de Physique du Globe de Paris, France

ABSTRACT: A stress determination campaign has been undertaken at the bottom of a 1200 m deep well located at Bramans, on the flanks of a mountain in the French Alps. The Hydraulic Tests on Preexisting Fractures (HTPF) method was chosen for it provides means to determine the complete stress tensor. The campaign was performed with a specific probe, coupling hydraulic straddle packers and an electrical imaging device. The on site processing of electrical data provide means to select and reoccupy precisely the various test zones. Analysis of the electrical signal recorded during the hydraulic tests was found to exhibit a characteristic signature during fracture closure or fracture reopening. Hence normal stress magnitudes have been determined thanks to both the electrical and the hydraulic signature of fracture opening and fracture closure. Results show that none of the principal stress components is vertical.

In august 2000, the stress tensor at the depth of a future tunnel was determined with the Hydraulic Tests on Preexisting Fractures (HTPF) method. The borehole was drilled near Bramans, a village located in the Maurienne Valley (French Alps). Its configuration introduced some difficulties : the 1200 m−long borehole was inclined 17° from the vertical and it intersected salt veins. This altered the response of the electric imaging device. The processing of the electrical signal had to be modified. Once this task was completed, borehole logging and hydraulic tests at a depth of 1100 m were completed by the same shift within 3 days.

As for most hydraulic fracturing stress measurements, the preliminary interpretation relied on pressure and flow rate data only. Various techniques are proposed to interpret hydraulic data : simple tangents method provides on-the-field values, while statistics give a better precision [1]. But these methods sometimes yield contradictory results and the choice of the pertinent hydraulic method has been extensively debated [5].

Complementary independent data may constrain further the value of the shut-in and reopening pressure. For this reason, the electrical data recorded by the imaging device were quantitatively examined. We then discovered that they undergo major changes during a hydraulic test. Discussions of these electrical data and their integration into a systematic measurement methodology are presented in this paper.

1. HPTF METHOD AND TOOL

1.1. *Principles of the HTPF Method*

THe HTPF method consists in performing multiple hydraulic tests on preexisting fractures with various orientations[3]. The stress tensor $\overrightarrow{\overrightarrow{\sigma}}$ is obtained from the following system of equations:

$$\sigma_n^i = \vec{n}_i \cdot \overrightarrow{\overrightarrow{\sigma}} \cdot \vec{n}_i \,. \tag{1}$$

where $\vec{n}_i$ labels the vector normal to the plane of the i^{th} tested fracture and σ_n^i denotes the normal stress applied on this fracture. Note that there is no assumption on the principal direction in this system and that this method is still valid in complex environments where all six components of the stress tensor are needed.

The procedure of a HTPF campaign is as follows:

- **(i)**. The borehole is logged and preexisting fractures amenable for testing are identified.
- **(ii)**. *Each* selected preexisting fracture is alternatively hydraulically reopened and closed. σ_n^i is then taken to be equal to the water pressure for which the fracture walls barely touch each other.
- **(iii)**. After *each* test, an electrical image of the borehole yields the orientation of the reopened fracture $\vec{n}_i$.

As seen in Eq. (1), at least six independent equations are needed to determine the full stress tensor but usually more tests are conducted to increase the accuracy of the stress determination and to limit effects of

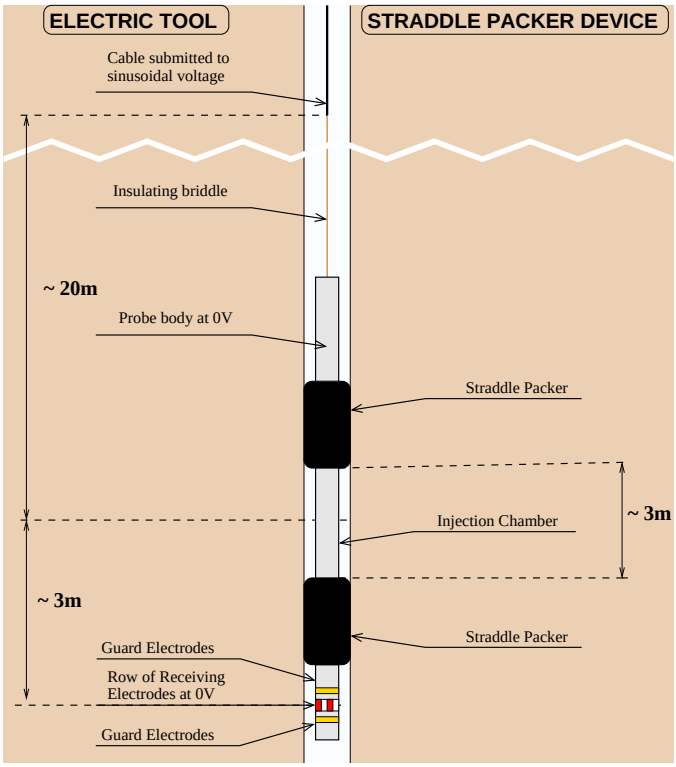

Fig. 1. Schematic representation of the HTPF-40 probe.

stress heterogeneities. If a large portion of the borehole is investigated, the stress gradient may also be computed, if at least 12 measurements are performed.

1.2. *The HTPF Tool*

The HPTF tool is a tool specially designed for HTPF stress measurement campaigns. Over more than 10 years, different versions of this tool have been developed and used. The tool presented here, and exhibited on Fig. 1, is the slim borehole version (2.5 inches in diameter).

Each HTPF tool is a wireline hybrid probe offering at least two functionalities:

- a hydraulic straddled packer system
- an electrical imaging tool, based on Mosnier's concept[6], from which Schlumberger's FMI and FMS logging tools have been derived.

The electric tool fulfills tasks (i) and (iii) of a HTPF campaign, while the hydraulic component is used to measure reopening and shut-in pressures and carry out task (ii).Thus, only one tool is displaced along the borehole, whithout a need for a drilling machine.

The hydraulic equipment includes two injection lines. The first one monitors the pressures inside inflatable packers. The second injects clear water in the straddled section and within the fracture, once it is opened. Fluid pressure at the level of the test chamber is monitored with an accuracy at about 0.1 %. Flow rate is recorded at ground surface.

The electric tool is composed of an injection electrode (the logging cable), a 20 m−isolating bridle and a row of reception electrodes. The logging compartment includes the reception electrodes and the electronic recording system. For slim boreholes, the 24 receiving steel electrodes are set on a row located 3 m below the test chamber, in contrast to the tool for larger boreholes for which 10 rows of 16 electrodes are set within the straddled interval. This restriction considerably alters the precision of the fracture orientation : the theoretical horizontal angular precision is only 15°. However during logging, the multiplicity of sampled cross-sections improves this precision up to $7-8°$. As logging is performed with a displacement rate of 2 m/min, the vertical resolution is about 0.7 cm.

2. ELECTRICAL MONITORING WITH THE IMAGING TOOL

As the imaging tool is devoted to fracture orientation determination, little attention has been given up to now to the quantitative interpretation of the electric signal. This situation changed during the Bramans campaign, as salted water and inclined borehole required signal processing of the row images.

2.1. *Pressure-Correlated Electrical Variations*

A study of electrical signals revealed that their intensity was varying during the tests, although the reception electrodes were located 3 m below the straddled interval.

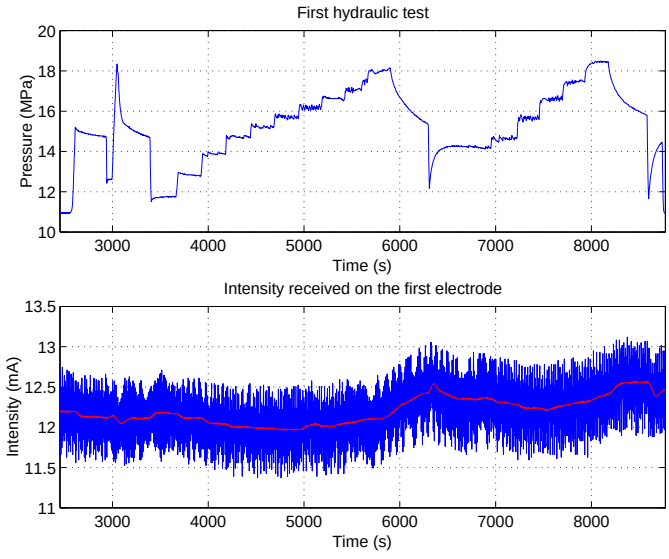

Fig. 2. Variation of the intensity received on one electrode during the first hydraulic test. The overlaid solid line displays the filtered signal.

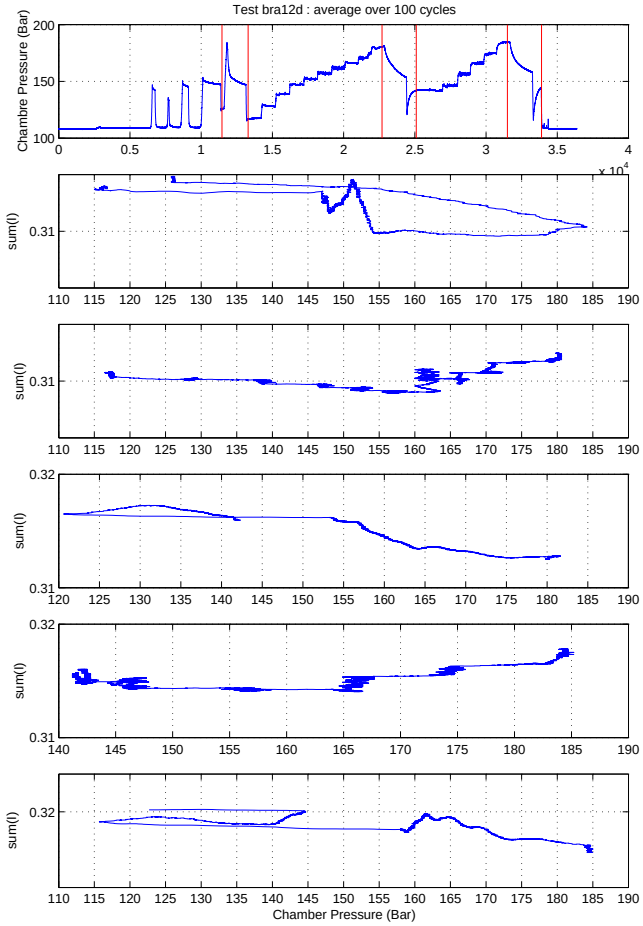

Fig. 3. Variation of the sum of the currents received by the 24 electrodes during the first test of the Alps campaign. Electrical data are averaged over 6 s. The upper figure displays the variation of chamber pressure with time, while the five lower ones are pressure versus electrical current curves for each step. Closure and reopening of the fracture is expected to induce sharp variations in the electric current and its derivative. The shadowed zones highlight the fracture reopening and shut-in, identified by hydraulic methods.

Figure 2 displays the intensity collected by one electrode during the first hydraulic test. The displayed signal is very noisy but the noise is quite coherent and regular; low-pass filtering enables to track its fine variations. As this variation amounts to about 1 % of the signal, it is therefore to be considered with caution.

To verify the efficiency of the coupling, chamber pressure and electrical current are cross-plotted such as in figure 3. All five measurement sequences are displayed : sub-figures (1), (3) and (5) correspond to shut-in of the fracture and the two others to reopening sequences. The electrical current displayed in this figure is the sum of the currents collected by all the electrodes, after low-pass filtering of 6 s-cut-of period.

These curves exhibit sharp inflexion points, especially the first, second and fourth ones. These sharp variations occur within the confidence intervals of the normal stress hydraulic measurements, delineated by the shadowed area. This suggests that these changes in slope are hydraulically pertinent.

However, during the last two shut-in tests, numerous variations are noticeable, both before and after the hydraulic closure of the fracture. Analysis of the signal received by all 24 electrodes enables to select the most pertinent inflection point. Figure 4 corresponds to such a study for the second shut-in sequence. The variety of behaviors displayed is striking : electrodes 1 to 6 show little variation while 7 to 23 display acute variations at 16.4 MPa, in accordance to hydraulic values. Other variations are also perceptible at 17.0 MPa but they are less pronounced and correspond to sharp variations only for electrodes 16 and 17.

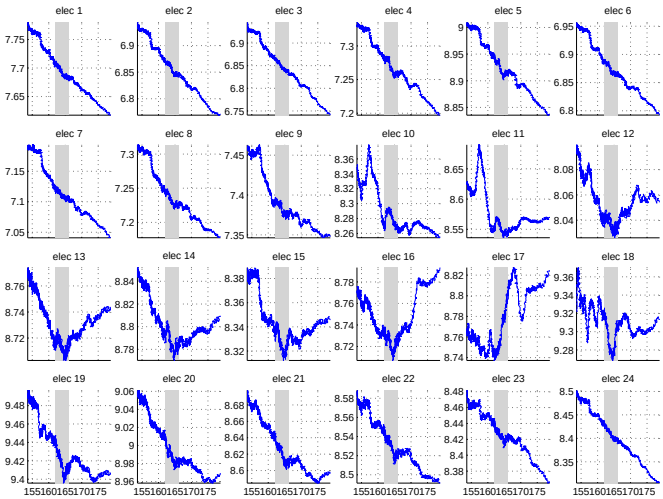

Fig. 4. Electrical data collected by each electrode during the second shut-in (period (3) of figure 3)

2.2. *Interpretation of the Signal Variations*

Similar analogous variations of the electrical and pressure data appear in the vast majority of the hydraulic tests performed with HTPF probe during the last 10 years. The origin of these variations is therefore either mechanically significant or systematically introduced by the tool.

The variation of the electric signal can grossly be linked to three factors :

- Probe perturbation: it can move, and there can be variation in electric injection.
- Borehole variation : the fluid inside the borehole becomes less saline as the hydraulic test proceeds.
- Surrounding rock interaction, and especially the tested fracture, which goes down up to the level of the receiving electrodes.

The first cause is potentially the most significant. During the same campaign, excentering effects indeed amounted to about 50% of the signal and blurred the image. It is thus expected that a slight movement of the tool may induce an important change in the received current. However during the hydraulic test, the tool is tightly packed to the borehole walls. This is confirmed by the tilting sensors, precise to 0.1°, which do not detect any change in the tool position. The effect of a possible tool motion is thus discarded.

The second cause is difficult to estimate. Packers are built according to an auto-blocking system, so that the volume of the chamber varies during the test. Moreover, the salinity of the fluid trapped by the chamber pressure evolves as clear water is injected.

The third cause is the most promising, provided it is not overshadowed by other secondary factors. During logging, the passing of reception electrodes in front of a fracture induces a typical variation of 50% of received electrical intensity. But during the test, the fracture is located 3m below the straddled interval. However, during the tests, the volume injected inside the test chamber is equal to about 20l. As the chamber volume is about 10l, this suggests that the fluid propagates along a fair distance inside the fracture, and the electrical signal becomes more sensitive to the fracture opening. However, if the fracture is interconnected with a fracture network, the shape of the electric signal is likely to become also more complex. Such behavior is noticeable in Fig.3. Logs of the borehole region surrounding the tested fracture showed that this fracture was effectively intersected by other fractures.

The electrical signal is thus sensitive to the alterations which occurred in the rock and the borehole, and not in the tool itself. During a hydraulic test, these changes are induced by the fluid injection. Electric data then offer the opportunity to monitor the change in mechanical and hydraulic regimes during a test.

3. STRESS DETERMINATION THROUGH HYDRAULIC AND ELECTRIC METHOD

This coupling between pressure variation inside the chamber and the received current below the chamber suggests a new method for determining normal stress supported by the tested fractures.

3.1. *Stress Determination with Hydraulic Methods*

The normal stress applied to the preexisting fracture is determined through three steps :

- *A first breakdown stage*. The closed preexisting fracture is fully opened, then water injection stops and the fracture closes.
- *Two quasi-static reopening sequences*. Hydraulic pressure progressively increases until fracture reopens. Water injection is stopped some time later, and the fracture closes.

We determine a reopening pressure (P_r) and a shut-in pressure (P_s) for each step. The initial breakdown pressure is discarded, as it may be affected by cementation of the preexisting fracture; The normal stress applied to the fracture is therefore determined through a set of 5 values : 3 shut-in and two quasi-static reopening pressures. Reproducible values testify that the mechanical environment has not been substantially perturbed by the hydraulic experiment. This procedure then gives tight uncertainty intervals, thanks to the numerous values it deals with.

Hydraulic interpretation of the reopening curves point out the closure and reopening of a fracture as transitions between two limit regimes :

- As fracture is closed, flow rate and pressure gradient are linearly related through Darcy formula.
- As fracture is opened, Poiseuille flow occur between the two planes of the fracture. The relationship between pressure and flow rate is again linear and an effective permeability can be defined. This permeability is significantly higher than in the closed regime.

Quasi-static reopening procedure guarantees stable flow conditions before each pressure impulsion. The precision surrounding the flow rate values is therefore improved. Plotting flow rate versus pressure is then a direct and reliable way to determine reopening

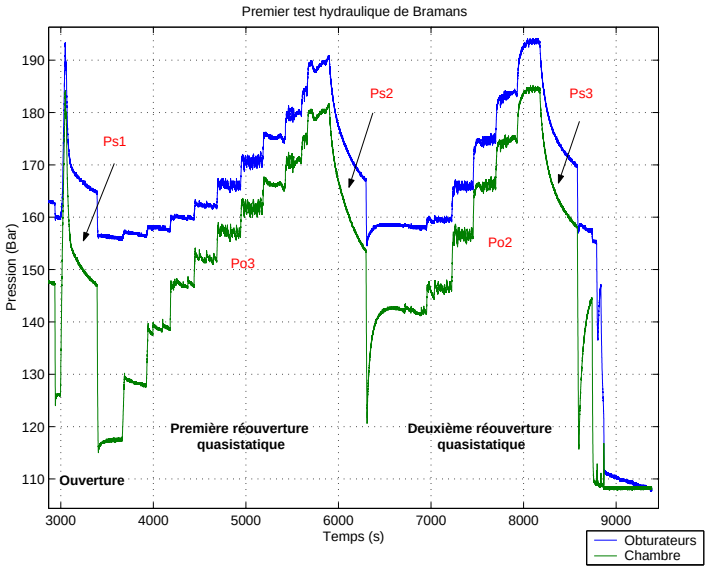

Fig. 5. Summary of the hydraulic method to determine stress procedure. The three steps of the test procedure are displayed. Below are examples of derived curves from which reopening pressure (on the left) and shut-in pressure (on the right) are determined

pressure.

The number of data points equals the number of steps in the reopening sequences. The experiment should be carefully designed to ensure at least three points are taken before and after the reopening, so that the limit straight lines are well defined. In practice the early departure of the data points from the limit tangent lines introduces a large transition interval which often alters the efficiency of the method.

For shut-in sequences, interpretation relies only on the variation of pressure with time. Various techniques have been proposed to extract shut-in pressure from this curve. The simplest one considers only the tangents at the beginning and at the end of the curves, as traced in Fig. (5). Intersection of the initial and final tangent lines yields acceptable results provided the shut-in period is not tool long as compared to injected volume. It is commonly done on the field. On the other hand, Aamodt ans Kuriyagawa attempt to interpret the whole curve by fitting with an exponential pressure-decay law [1].

In summary, hydraulic data are theoretically easy to interpret since only one inflexion point is to be evaluated. It corresponds to the closure or reopening of the fracture. But in practice, it is sometimes difficult to determine precisely because of the smoothness of the hydraulic data.

3.2. *Stress Determination with Electrical Method*

Hydraulic interpretation has been classicaly used for interpreting data acquired during HTPF campaigns. However, Fig.2 shows that sharp bends in electrical

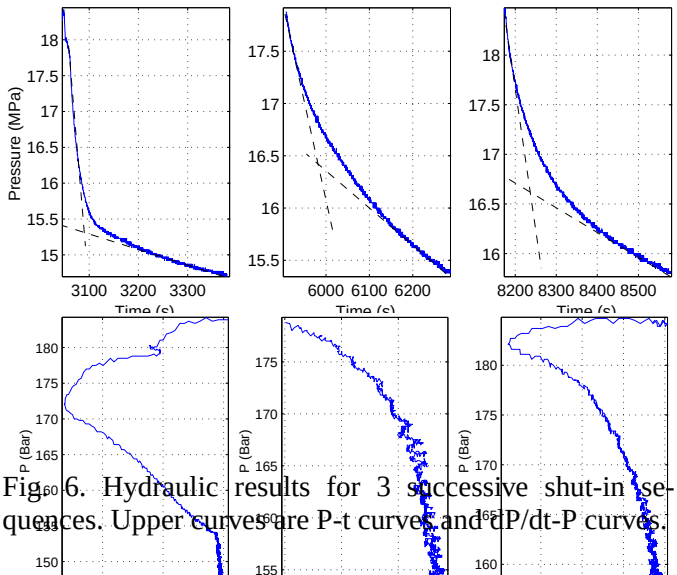

Fig. 6. Hydraulic results for 3 successive shut-in sequences. Upper curves are P-t curves and dP/dt-P curves.

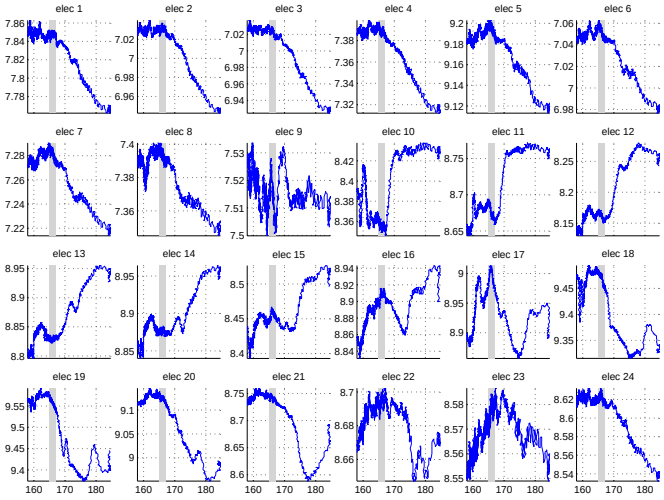

Fig. 7. Electrical data collected by each electrode during the third shut-in (period (5) of figure 3)

data occurred within the confidence interval of the closing and reopening pressure determined with hydraulic methods. *Supposing that these variations are indicative of closure and reopening of the fracture*, they give more precise values for normal stresses. Do these sharp inflections systematically yield the shut-in transition value ?

Quasi-static reopening stages are less amenable to study electrical data. They were designed to plot pressure versus flow rate curves and not to record continuous electrical data. While pressure is maintained constant, electrical data generally vary notably during the transient interval following the pressure surge. We will therefore focus on shut-in sequences.

Comparing many shut-in sequences give clues about the pertinence of the electrical technique. Almost all hydraulic tests which we conducted during these last 10 years present similar correlation between the electrical and hydraulic data. Many examples are therefore available to check the electric technique, but we will restrict our discussion to the data set presented in section 2. The three shut-in sequences seen in Fig. 3 correspond to the closure of the same fracture. The tool has not moved and the electrical data of the three shut-in sequences are comparable. The variety in behavior of the electrical data, already visible in Fig. 3, suggests that this sample is still pertinent to study the efficiency of the electrical method.

Following Baumgartner and Zoback [2], we computed hydraulic shut-in pressures with different techniques. First, the simple tangent methods are applied to pressure versus time curves. Second, shut-in pressures are also deduced from dP/dt versus time. The two estimations are presented in Fig. 6. As it is often noted, the two techniques give slightly different shut-in pressure values.

During the first shut-in, a sharp trend change at a pressure of about 15.4 MPa is visible on both hy-

draulic and electric pressure. The pressure-derivative curve is here the most precise and give a shut-in pressure of 15.4 ± 0.05 MPa. The trend on all electrode is similar and the sum of the collected currents displayed in figure 2 reflects well their variations. Electrical method gives a shut-pressure of 15.4 ± 0.1 MPa and is consistent hydraulic results.

The second shut-in sequence is more difficult to interpret. Hydraulic data do not exhibit any sharp inflection point. Electrical data exhibit many bends in Fig. 4. However, at 16.4 ± 0.05 MPa, a sharp bend is noted. Pointing this value is very easy, as for most electrodes, the inflection is in fact a minimum. The electrical data give therefore a very accurate shut-in pressure reading, provided the bend to pick up is identified.

Discrepancies between hydraulic and electric data occur in the third shut-in. Shut-in pressure is set to 16.6 ± 0.2 MPa thanks to the dP/dt-P curve. But electrical data displayed in figure 7 rather exhibit a major bend at 17.0 ± 0.1 MPa . A minor bend is also visible at 16.8 ± 0.1 MPa. Hydraulic data therefore suggest the bend to pick up is the second one.

In the end of section 2, we already noticed that the complex behavior the curves exhibit may be due to a branching fracture. This fracture appeared to pass near the electrode. The closure of this fracture may therefore explain the major bend. The minor bend at 16.8 ± 0.1 MPa would be linked then to the closure of the tested fracture, a feature which would be consistent with hydraulic data. This also may be a warning that the initial stress field may have been disturbed. This may explain the discrepancy between the first shut-in and the following shut-ins.

This case study highlights the difficulty in using electrical data by themselves when electrodes are outside the straddled interval. The strategy for using the electrical data is thus to integrate them to otherwise acquired hydraulic data. The accuracy summary displayed in Fig.8 suggests that handling electrical data may be worthwhile. Inverse problem theory is an easy way to integrate hydraulic and electrical data.

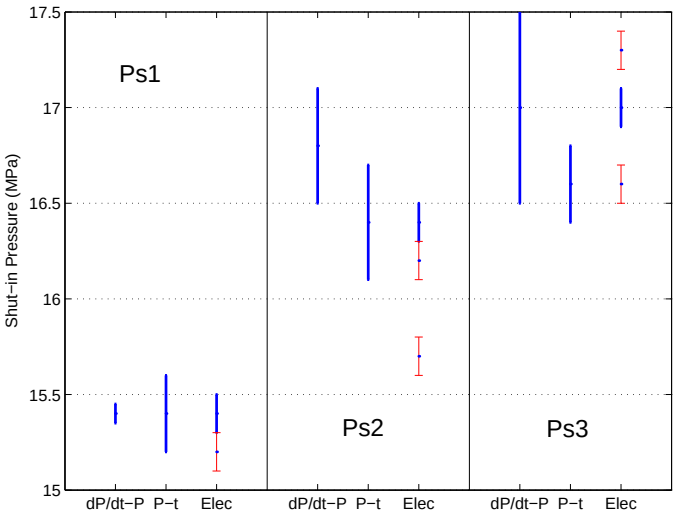

Fig. 8. Shut-in pressure estimations from dP/dt-P, P-t and electric responses, for each shut-in sequence. Thick lines denotes major bends and thin lines minor bends.

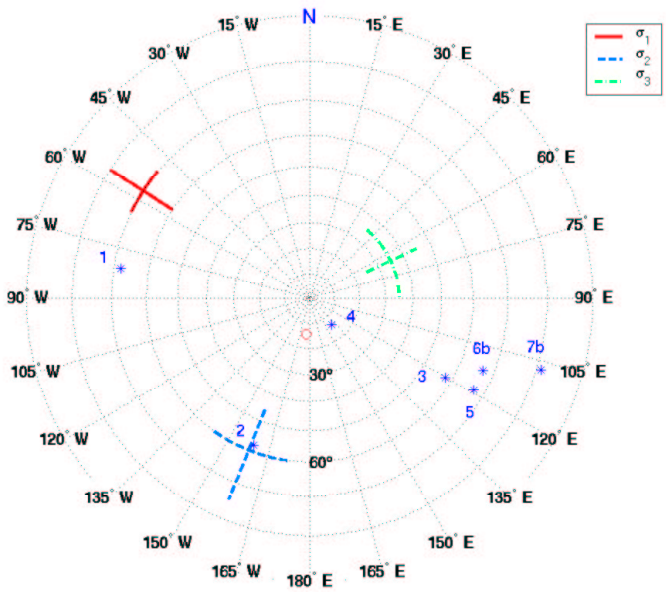

Fig. 9. Orientation of of the stress principal directions. The vectors normal to the tested fractures are denoted with stars, while the direction of the tilted borehole is indicated by the black circle.

4. INTEGRATING ELECTRICAL DATA IN STRESS DETERMINATION SCHEME : APPLICATION TO THE BRAMANS CAMPAIGN

Fig. 9 is a stereographic diagram displaying the principal stress directions. The orientations of the normal to the tested fracture are also indicated with stars. Their repartition is not homogeneous : tests 3, 5, 6*b* and 7*b* dips to about 70° with a mean azimuth of $N120°E$. The inversion of Eq. (1) is therefore extremely sensitive to the accuracy of the data collected in tests 1,2 and 4.

Electric data are available for tests 1 and 2 (later tests were altered by a deficiency in the electronics). We have already extensively dealt with the first test in the previous section. How can Fig. 8 be quantitatively integrated in the inversion process ?

4.1. *Generalized Inverse Problem Theory*

The probabilistic formulation is an easy way to integrate both electric and hydraulic method. In this approach, uncertainties surrounding the data are described as Probability Density Functions (PDF). The

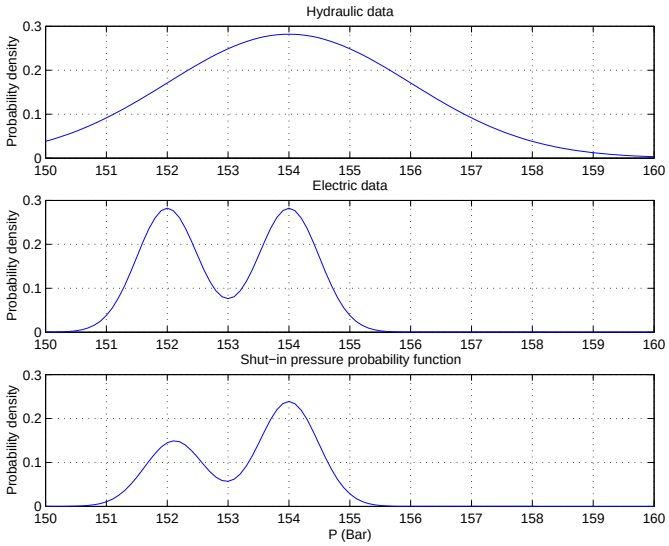

Fig. 10. Principles of the integration of hydraulic and electric data inside a signal probability function, dealt with help of Tarantola's inverse problems theory.

PDF of inversion results can be deduced from the PDF of the experimental data thanks to the formulas demonstrated by Tarantola [7].

Gaussian PDF are calculated from the error-bars presented in Fig. 8. These error-bars correspond to a 95% confidence level, so that the standard deviations amount to 6 times their width. If electrical data have many bends, the Gaussian function are summed and normalized : this mathematical treatment is equivalent to a logical OR, as used in computer science. Pondering factors can be introduced to differentiate minor and major bends. Two typical PDFs are drawn in the upper axes of Fig. 10

We can then compute the PDF of normal stress value. The logical AND is described with a multiplication of the hydraulic and electrical PDF. The normalized resulting PDF is similar to the function depicted on the lower axis of Fig. 10. This function is more precise than the original PDFs : its width is lower than for hydraulic data while the higher peaks correspond to the electrical bend which is the most consistent with hydraulic values. We have then extracted information from both types of data. Note that the maximum of the resulting PDF is different from the maxima of the initial PDFs.

The main drawback of the generalized inverse theory is its computation cost. In practice, computation are led with least-squares method. Tarantola and Valette demonstrated that this method could be derived from the generalized inverse theory under simplifying assumptions.

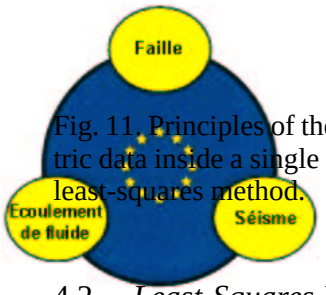

Fig. 11. Principles of the integration of hydraulic and electric data inside a single Gaussian function, to be used with least-squares method.

4.2. *Least-Squares Method*

Cornet and Valette adapted least-squares method to HTPF stress determination [4]. The main assumption underlying this method is that PDFs are Gaussian functions. The scheme presented in the generalized case, is then not directly usable. The PDF we get in the previous section can be used to shape a good Gaussian representation of the uncertainty surrounding normal stress value.

We propose to restrict the PDF to a Gaussian function centered on the highest peak described previously, as depicted in Fig. 11. Its width is the width of this peak. We lost information on the second peak but the final uncertainty is lower than for hydraulic data alone.

The numerical program used to interpret HTPF data implements a least-squares method. Uncertainty on the results are computed with Monte-Carlo algorithm. The principal stress components determined with Bramans data are reported on Table 1.

As it is noticeable in Fig. 9, the vertical direction is not a principal stress direction. This is due to topographic effects introduced by the flank of the valley.

Table 1. Stress principal components

	Intensity (MPa)	Azimuth (°)	Dip (°)
σ_1	27.5 ± 2.9	65 ± 25	35 ± 10
σ_2	22.5 ± 2.5	-158 ± 15	60 ± 15
σ_3	15.0 ± 1.4	-57 ± 7	70 ± 10

5. CONCLUSIONS

When the HTPF probe is used for measuring the normal stress acting on preexisting fractures, electrical data display variation in phase with the variation in hydraulic signal. Similar variations have been observed for all the previous campaigns, performed in different lithologies and stress environments.

These sharp inflections correspond generally to the shut-in pressure. However, electrical signals recorded by electrodes located some 3 m below the chamber test appear to be quite complex. and in practice, comparison with hydraulic data is compulsory. Similar studies conducted on results obtained with HTPF probes for which the electrodes are within the straddled interval show that the electric coupling is much stronger and well-correlated with the pressure transients. This increases our confidence in the physical meaning of intensity variation observed at Bramans.

This highlights the usefulness of the electric component of the HTPF probe. Besides identifying the orientation of the preexisting fractures, it improves the accuracy of the normal stress determination. It shortens significantly the duration of HTPF campaign with important economic consequences.

Acknowledgments – The Bramans stress determination campaign was conducted for Alpetunnel in the context of the reconnaissance for TGV tunnel. We thank sincerely Alpetunnel for letting us use these data in this presentation.

REFERENCES

Aamodt, R. & M. Kuriyagawa 1983. Measurement of instantaneous shut-in pressure in crystalline rock. In *Hydraulic Fracturing Stress Measurements*, pp. 139–142. Washington D.C., National Academic Press.

Baumgartner, J. & M.D. Zoback 1989. Interpretation of hydraulic fracturing pressure-time records using interactive analysis methods. *International Journal Rock Mechanics and Mining Sciences*, 26(6):461–469.

Cornet, F.H. 1993. The htpf and the integrated stress detrmination methods," in "comprehensive rock mechanics. In Hudson, J.A. (ed.), *Rock testing and site characterization*, volume 3 of *Comprehensive Rock Engineering*, chapter 15, pp. 413–432. Oxford, Pergamon Press.

Cornet, F.H. & B. Valette 1984. In situ stress determination from hydraulic injection test data. *Geophy. Res. Lett.*, 89(B13):11527–11537.

Haimson, B.C. 1993. The hydraulic fracturing method of stress measurement–theory and practice. In Hudson, J.A. (ed.), *Rock testing and site characterization*, volume 3 of *Comprehensive Rock Engineering*, chapter 14, pp. 395–412. Oxford, Pergamon Press.

Mosnier, J. & F. Cornet 1989. Apparatus to provide and image of the wall of a borehole during a hydraulic fracturing experiment,. In Louwrier, K., E. Staroste & V Garnish, J.D.and Karkoulias (eds), *4th international seminar on the results of EC geothermal energy research and demonstration, proceedings*, pp. 205–212. Commission of the European Communities, Kluwer Academic Publishers.

Tarantola, A. 1987. *Inverse Problem Theory*. Elsevier.